JOURNAL OF OPTOELECTRONICS AND ADVANCED MATERIALS Vol. 9, No. 11, November 2007, p. 3411 - 3414

The matrix effect on spectrochemical analysis accuracy of AISI 316 biomaterial grades

I. PENCEA[a*], M. BRANZEI[a], F. MICULESCU[a], M.PENCEA[b], O.TRANTE[a], M. MICULESCU[a]
[a]*University Politehnica of Bucharest,*
[b]*"Viaceslav Harnaj" Lyceum, Bucharest Romania*

The accuracy and precision of spectrochemical analysis of metallic biocompatible grades, especially AISI 316 grades, should be superior to the routine ones because they must fulfill rigorous chemical composition specified by ISO 5832-1 standard. As it is known, the atomic emission spectrometry (AES) is the most used technique in instrumental elemental analysis of metallic materials due to its high ratio efficiency-cost. But, exactneess of AES spectrochemical analysis of 316L grades depend on some critical factors as: sample microstructure; nature, size and distribution of inclusions; inter elements interferences, sample preparation etc[1,2]. This is way the ISO 5832-1 doesn't recommend AES for complete elemental analysis of 316L D and E alloy types.

(Received March 23, 2007; accepted November 1, 2007)

Keywords: Matrix effect, AISI 316, Spectrochemical analysis, Biomaterial

1. Introduction

The matrix effect consists in preferred initiation of micro spark discharge by the inclusions, grain boundaries or other inhomogeneities that induce systematic error in AES analysis [1-3]. There are methods to minimize matrix effect as the isoformation of analyzed area by high energy pre-sparking (HEPS), called microfusion, high rate repetitive sparking (HRRS) or macrofusion.

We investigated the matrix microfusion of an AISI 316 grade using a Foundry Master sparking stand in order to assess its effect on spectrochemical analysis exactness. The achieved data have had to prove that Foundry Master spectrometer can be used for spectrochemical analysis of AISI 316 alloys i.e. for charge preparation and for 316 grade identification.

2. Experimental

There were produced a batch of stainless steel 316 L bars (Φ~40 mm) to be used for implant manufacture. A lot of bars were forged (denoted F) and the other was cold drown (denoted CD). Samples cut of the middle of bars, 3 bars of each lot, were chemical, micro structural and SEM-EDS investigated. The elemental analyses were done by Spark Discharge in Argon using a Foundry Master spectrometer. The microstructure of samples were investigated by optical microscopy using a REICHERT UnivaR microscope equipped with an automatic line for image acquisition and processing. The inclusion content and morphology of the burned spots were investigated by optical microscopy using an Olympus SZX 2 microscope. The same morphologies of the burned spots were SEM investigated using a XL-30-ESEM TMP electron microscope. To asses the nature of byproducts formatted during sparking we used the Energy Dispersive Spectrometry (EDS) facilities of the XL-30-ESEM TMP microscope. The specific samples preparations were done using Buhler and MLG 11 equipments.

3. Results and discussion

The elemental concentrations of the 314L alloy bar batch measured according ISO 5832-1 standard by an accredited laboratory is given in Table 1. The elemental concentration of the specimens sampled from each lot of forged and cold drawn bars were measured 10 times repetitively i.e. ten burning spots on the same surface of 40 mm in diameter. The average elements mass concentrations of forged lot and the dispersion of the individual concentration (experimental standard deviation (STDEV) and relative standard deviation (RSD)) are given in Table 2 and Table 3. As it result from Tables 1-:-3 and Fig. 1. the spectrochemical analysis of 316L grade give close results to other chemical analysis made on the same grade according ISO 5382-1 requirements. From fig. 1 one may conclude that spectrochemical analysis of 316L alloy is improper for P, S, Al but these elements are at the level of ppm's in this grade and they can be considered trace elements. At these concentrations P, S, Al and even C concentrations lay in the LOD regions on their calibration curves were data spreading is higher. The representative transversal microstructures of the forged and cold drawn bars are given in Fig. 2 and Fig. 3. The images in Fig. 2 and Fig. 3 were selected from many analysed microstructure fields.

Table 1. The concentrations of AISI 316 biocompatible grades[4].

Elements	C %	Mn %	Si %	P %	S %	Cu %	Ni %	Cr %	Mo %	V %	Al %	N
(% mass)	0.030	1.50	0.45	0.024	0.003	0.05	14.57	17.54	2.75	0.03	0.005	0.050

Table 2. The average mass concentrations, STDEV and RSD of the main elements of a forged 316L grade.

Elements	C %	Mn %	Si %	P %	S %	Cu %	Ni %	Cr %	Mo %	V %	Al %
(% mass)	0.029	1.43	0.48	0.026	0.004	0.048	14.23	17.81	2.76	0.031	0.006
STDEV[1]	0.003	0.02	0.01	0.005	0.002	0.006	0.02	0.03	0.02	0.005	0.002
RSD[2](%)	10.3	1.4	2.1	19.2	50.0	12.5	0.1	0.2	0.7	16.1	33.3

1-STDEV-Standard Deviation; 2-RSD-Relativel Standard Deviation

Table 3. The average mass concentrations, STDEV and RSD of the main elements of a cold drawn 316L grade.

Elements	C %	Mn %	Si %	P %	S %	Cu %	Ni %	Cr %	Mo %	V %	Al %
(% mass)	0.032	1.45	0.46	0.025	0.003	0.051	14.53	17.61	2.73	0.032	0.005
STDEV[1]	0.003	0.01	0.02	0.006	0.001	0.004	0.02	0.02	0.02	0.006	0.002
RSD[2](%)	9.4	0.7	4.3	24.0	33.3	7.8	0.1	0.1	0.7	18.8	40.0

1-STDEV-Standard Deviation; 2-RSD-Relative Standard Deviation

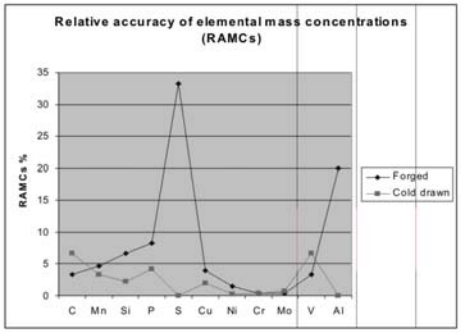

Fig.1. Relative accuracy of main alloying elements mass concentrations of the of a 316 L grade.

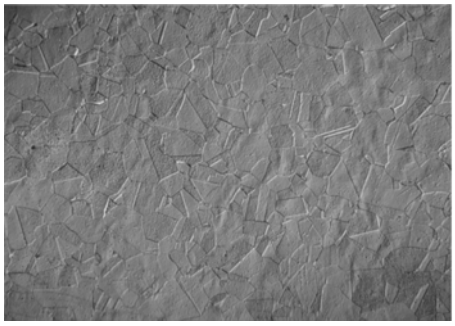

Fig. 2. Representative transversal microstructure of 316 L forged bars; X50.

The grain size of forged bars was evaluated at 6 after many grain fields assessed while cold drawn bars were evaluated at 5. From microstructural view point forged sample is more adequate for AES analysis than cold drawn sample because the grain limits is more uniform distributed across the sparking spot than cold drawn sample. But, Fig. 1 shows that spectrochemical data in the forged case are worse than cold drawn ones.

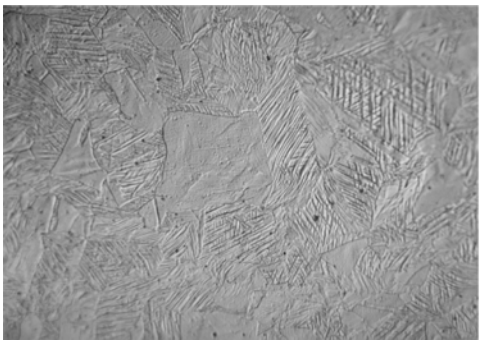

Fig.3. Representative transversal microstructure of 316 L cold drawn bars; X50

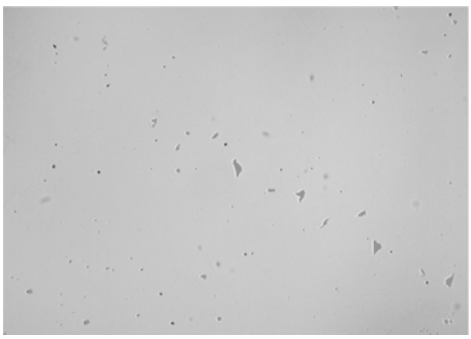

Fig. 4. a) Oxide inclusion distribution on the surface of a forged 316 L analysed sample; x20

One explanation of this misfit could be the large spreading of inclusions on the surface of analysed samples as could be seen in Fig. 4 and Fig. 5. The statistics in Fig. 4 b) show that the entire area of oxide inclusions is about 0.33 % of total area of Fig. 4a). The same the relative area of oxide inclusions in Fig. 5a is 0.13%.

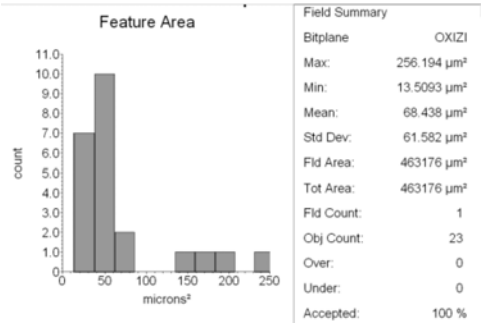

Fig. 4. b) Oxide inclusion statistics associated to Fig. 4 a.

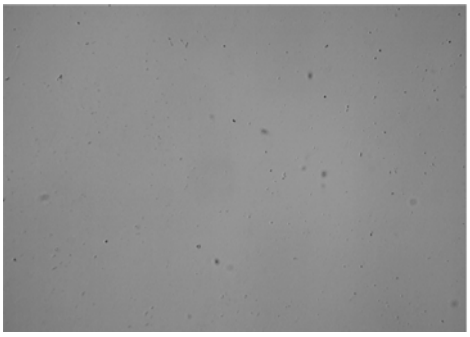

Fig. 5. a) Oxide inclusion distribution on the surface of a cold drawn 316 L analysed sample; x20

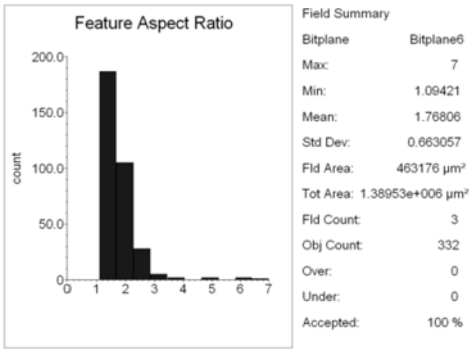

Fig.5. b) Oxide inclusion statistics associated to Fig.5a

The morphology and surface distribution of oxide inclusions could explain the higher scattering of spectrochemical data obtained on forged sample relative to the cold drawn ones. But, the HEPS pre-sparking and measuring sparking could consists in isoformation of sparking area, often called burn spot. In this sense, the presparked spots were optical investigated and were found that no morphological differences exists between forged and cold drawn samples as it is shown in Fig. 6 and Fig. 7.

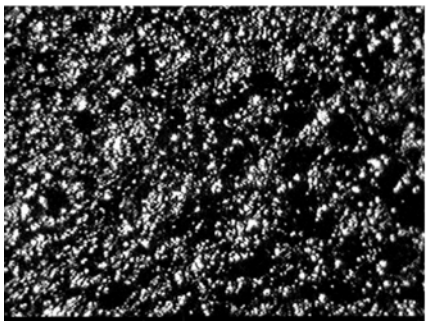

Fig. 6. Preburn spot image a forged 316 L sample.

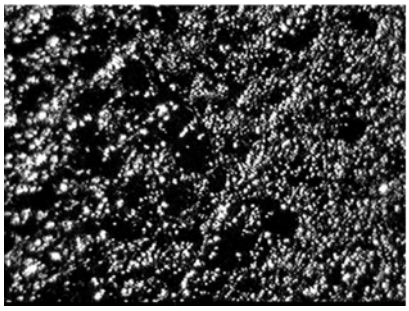

Fig. 7. Preburn spot image a cold drawn 316 L sample.

The SEM investigations have shown a surprisingly fact i.e. while optical stereomicroscopical images of burn spot morphologies looks like the SEM images at higher magnification differ on the place they were taken from the same spot. Thus, it worth analysing the morphology of a individually sparked spot rather than comparing burn spot morphologies on two sample with different microstructures. As it is shown in Figs. 8-:-12 the sparked spot morphology is complex. Thus, the burn spot of about 10 mm in diameter can be divided in three concentric regions as follows: central of about 3 mm in diameter; median disk sector of about 3 mm width and peripheral disk sector of about 4 mm width (Fig. 8). The rough surface shown in Fig. 8 hides the local effects of electric spark discharge that consist in local melting poles in the median zone (Fig. 9) and entirely melted central area of burned-spot (Fig. 10). The melt in Fig. 10 has frozen very fast.

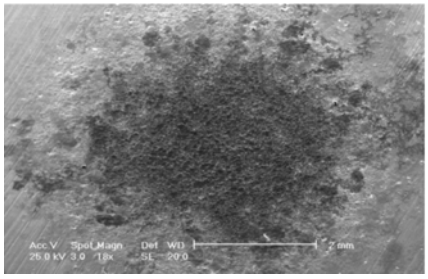

Fig. 8. SEM image of a sparked area on a forged specimen.

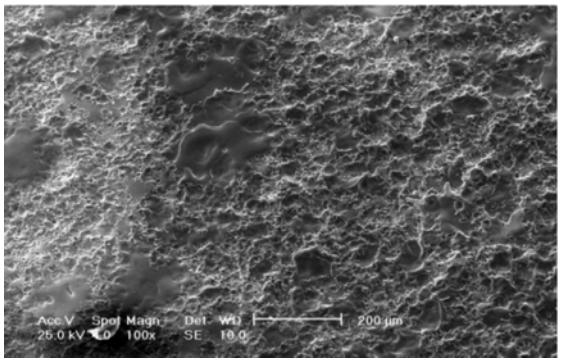

Fig. 9. SEM image of a median zone of the burned area shown in Fig. 8.

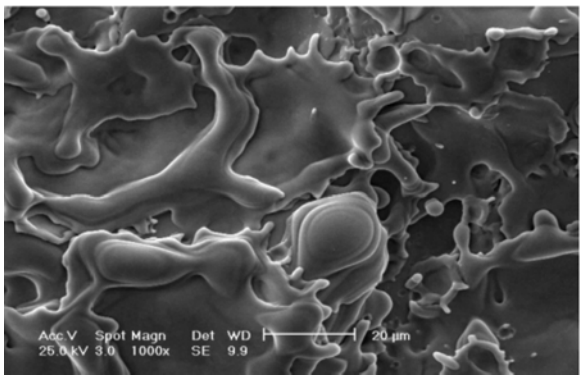

Fig. 10. SEM image of a central field of the burned area shown in Fig. 8.

EDS analyses on sparked spots showed that no unexpected burning products appear on sparked area as it is illustrated in Fig. 11. The above SEM images and many similar ones obtained by authors suggest that spark mechanism of spark discharge described by K. Slickers [1] could be reformulated as follows:

1. The spark discharge consists of many streamers that impinge on specimen sample.
2. When streamer strike a virgin place it causes local vaporisation or scattering of sample atoms
3. In the central zone of sparking spot impinge much more streamer, firstly due to geometrical factor of sparking stand and secondary due to rapid heating of central zone and thermal electron emission. Practically, the isoformation of the central spot zone is done by pre-sparking.

The median and outer zone of sparking spot remain more or less unisoformated and, in the same time, responsible for matrix effect on spectrochemical analysis.

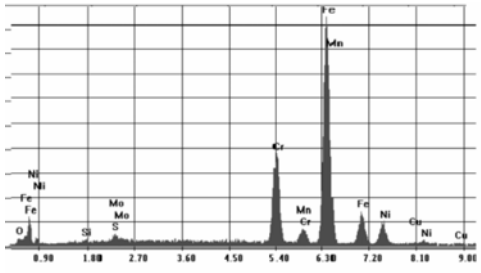

Fig. 11. EDS analysis on burned area shown in Fig. 8.

4. Conclusions

Our data prove that the sample suffers local melting during sparking and the sample's mass transferred into analysis gap is mainly vaporized and less scattered by ion etching. The authors explain the sample mass transferred into analysis gap on the basis of streamer theory. The streamer causes a very fast local melting and, subsequently, formation of a bubble of metallic vapor that explode with supersonic speed. The vapor are thermally excited and emit light among their spectral lines. It worth sense to accept that the bubble explosion causes melt splat, rather metallic cluster splat. We consider that the cluster aggregation and vapor desublimation (Fig. 10) that presents micro dendrites on the burn-off area. To avoid matrix effect in 316L spectrochemical analysis the sample should be previously macro fused, when it is possible!

Acknowledgements

This work was partially supported by The National University Research Council of Romania under Grant 477-2005 and partially by PNCD-CEEX under Grant 2673-2006.

References

[1] K. Slickers, Automatic Emission Spectroscopy, Bruhldruckerei, (1986).
[2] I. Pencea, Basics of spectrochemical analysis by optical emission in ark and spark discharge, Printech, 2007
[3] P. Holler, K. Slickers, H. Matter, Stahl und Eisen **189**, 948 (1989).
[4] I. Pencea, Material's structure analysis basics, Printech (2001).
[5] N. Barbulescu, R.Titeica, D.Barca-Galateanu, I.Spanulescu, L.Georgescu, Physics, v. I, Ed. Didactica si Pedagogica (1972).

*Corresponding author: ipencea@yahoo.com